Hindawi
Journal of Chemistry
Volume 2020, Article ID 2150419, 10 pages
https://doi.org/10.1155/2020/2150419

Research Article

Synthesis of Mixed Ligand Ruthenium (II/III) Complexes and Their Antibacterial Evaluation on Drug-Resistant Bacterial Organisms

James T. P. Matshwele,[1] **Florence Nareetsile**,[2] **Daphne Mapolelo**,[2] **Pearl Matshameko**,[3] **Melvin Leteane**,[3] **David O. Nkwe**,[4] **and Sebusi Odisitse**[1]

[1]*Botswana International University of Science and Technology, Department of Chemistry and Forensic Sciences, Private Bag 16, Palapye, Botswana*
[2]*University of Botswana, Department of Chemistry, Private Bag 0704, Gaborone, Botswana*
[3]*University of Botswana, Faculty of Science, Department of Biological Sciences, Private Bag 0704, Gaborone, Botswana*
[4]*Botswana International University of Science and Technology, Department of Biological Sciences and Biotechnology, Private Bag 16, Palapye, Botswana*

Correspondence should be addressed to Sebusi Odisitse; sebusi.odisitse@gmail.com

Received 6 December 2019; Revised 20 February 2020; Accepted 22 February 2020; Published 19 March 2020

Academic Editor: Marcelino Maneiro

The potential antimicrobial properties of a tridentate polypyridyl ligand 4-butoxy-*N*,*N*-bis(pyridin-2-ylmethyl)aniline (BUT) 1 and its corresponding mixed ligand ruthenium complexes were investigated on drug-resistant and non-drug-resistant bacterial species. The ligand and its complexes were synthesized and successfully characterized by ^{1}H NMR, UV/Vis, and FTIR spectra; ESI-MS; and magnetic susceptibility. Electronic spectra and magnetic susceptibility of these Ru(II)/(III) complexes suggest that they are of a low spin crystal field split, where the Ru(III) is a d^5 and Ru(II) d^6 low spin. These compounds were tested for antibacterial activity on two bacterial species: *Staphylococcus aureus* (*S. aureus*) and *Klebsiella pneumoniae* (*K. pneumoniae*), as well as their drug-resistant strains methicillin-resistant *Staphylococcus aureus* (MRSA) and multidrug resistant *Klebsiella pneumoniae* (MDR *K. pneumoniae*). All the compounds inhibited growth of the two non-drug-resistant bacteria and only one drug-resistant strain MRSA. However, only the ligands BUT and 2,2-dipyridylamine showed activity against MRSA, while all complexes did not show any antibacterial activity on MRSA. We observed large zones of inhibition for the Gram-positive *S. aureus* and MRSA bacteria, compared to the Gram-negative *K. pneumoniae* bacteria. DNA cleavage studies with gel electrophoresis showed denatured bacterial DNA on the gel from all the complexes, with the exception of the ligand, suggesting DNA nuclease activity of the complexes in the bacterial DNA.

1. Introduction

Antibiotic resistance is a growing public health issue that may lead to epidemics of drug-resistant bacterial species. It has been realized that there are various possible targets for inhibiting bacterial infection, with one of them being attacking the bacterial genomic material [1]. The issue of drug resistance by bacterial infections has become a major problem in global public health, such that in 2014 the World Health Organization (WHO) acknowledged the lack of antibiotic development in the last 25 years. Effective antibiotics have decreased in numbers, thus making resistant bacterial infections be topical health issues [2]. In this regard, medical researchers have been putting more effort to address this issue. Literature shows a shift from conventional organic based antibiotics to metal-based drugs as these show promising results over broad range of microbial infections. In this paper, we investigate the potential of ruthenium-based antibiotics against non-drug-resistant bacterial strains and drug-resistant strains.

The biological application of ruthenium has increased over the years, especially after the realization of this metal's important bioactive properties which include anticancer, antimicrobial, and antiviral properties [3–8]. Ruthenium complexes also have some interesting chemical and physical properties which make them good candidates as potential drugs. These complexes are known to be borderline between hardness and softness, which allows them to form strong chemical bonds with a series of elements of different hardness and softness. Thus, this property allows ruthenium to bind to a variety of biomolecules including the genomic material [9]. One other important feature of ruthenium is that it can access a series of oxidation states (II, III, and IV) due to its low interconversion energy barrier [10]. This flexibility in oxidation state gives rise to a slow ligand exchange rate, which would translate into these complexes having good affinity to biomolecules. Thus, as they lose their labile ligands, stronger donor atoms from the biomolecules would fill the gap they left in the coordination sphere of ruthenium [11]. Kinetics of the ruthenium complex on a time scale of mitosis have been studied, and it was found that, when it binds to the cell, it is more likely that the ruthenium complex will remain in the cell for the entire life course of the cell [12]. Ruthenium is directly below iron in the periodic table, and it has been observed that ruthenium tends to have iron mimicking properties when bound to biomolecules. Consequently, if there is ruthenium poisoning due to destabilization of these complexes, the body responds in a similar manner to iron poisoning [12].

With all these interesting properties of ruthenium, the choice of the ligand is very important and must be rational. This is because there are ligands that either mute, enhance, or basically make these properties present. This has a negative or positive effect on the target bacterial organism or biological function [11]. The most common choice of ligands is either the Schiff base ligands [13–16] or heterocyclic polypyridyl ligands, with the latter being the most common [17–22]. Polypyridyl ligands have one or more pyridine rings, and these are important ligands in coordination chemistry. These ligands tend to induce the chemical and even the physical properties of various metal centres. These properties include the photophysical properties which give rise to the characteristic metal to ligand and ligand to metal charge transfers. This property gives rise to the characteristic crystal field split that gives the characteristic color and electronic transition energies of various polypyridyl complexes [23]. These ligands are also known to be lipophilic in nature, which allows for easier cell access because the lipopolysaccharide layer (LPS) is made up of fats, which then makes these ligands be more attracted to these cellular membranes. This means that the hydrophobic nature of these ligands can facilitate entering the cell as they would interact well with the LPS [24]. Intercalation in biochemistry is a process where a compound fits itself between planar base pairs of double stranded genomic material. This is a physical binding process of compounds to genomic material. It is a process that is being widely used to explain some of the mechanisms and proposed mechanisms of actions of some potential drugs. Examples of intercalators are aromatic planar polycyclic organic molecules which include heterocyclic polypyridyl group of molecules [11, 25]. This is one other important reason for the choice of these polypyridyl ligands in terms of increasing the chances of these ruthenium complexes in disrupting the cellular processes of these bacterial cells.

As evidenced by the above literature, compounds of ruthenium and polypyridyl ligands are potential bioactive agents for various diseases. Thus, in this study, we explored the synthesis of a new ligand and its ruthenium complexes. We further investigated their potential antibacterial efficacy against the two bacterial species *Staphylococcus aureus* and *Klebsiella pneumonia* together with their drug-resistant strains. This was assessed through preliminary tests and DNA cleavage studies.

2. Experimental

2.1. Materials and Instrumentation. All chemicals for synthesis and biological activity reagents were purchased from Merck Sigma Aldrich (USA) and used without further purification. The neat film infrared spectroscopy of the compounds was recorded in the 4000-500 nm region using a PerkinElmer System 2000FTIR spectrometer (Perkin Elmer USA). UV-Visible absorption spectra were recorded in 1 cm path length quartz cells at room temperature, using a Shimadzu UV-31-1 PC scanning spectrophotometer (Shimadzu Corp, Japan). HRESI-MS data were acquired using Waters UPLC XEVO G2-XS QTof system. The acquisition parameters were as follows: drying gas was at 50 L/h at 150°C drying gas temperature, the desolvation gas was 591 L/h and at 300°C, and capillary voltages were at 2.49 kV (Waters Corp, USA). The data were processed on MestreNova version 9.0.1-13254.

2.2. Synthesis. The 2,2-dipyridylamine ligand was purchased from Merck Sigma Aldrich (USA). The synthetic scheme for the synthesis of the ligand and all the complexes is shown in Figure 1.

2.2.1. Preparation of 4-Butoxy-N,N-bis(pyridin-2-ylmethyl) aniline (BUT) (1). 4-Butoxyaniline (160 mg, 0.97 mmol) and 2-chloromethyl pyridine (320 mg, 1.93 mmol) were dissolved in 10 ml of 1 : 1 acetonitrile to water solvent mixture. The mixture was refluxed while 5 ml of NaOH (780 mg 1.93 mmol) was added over a period of 30 min. The reaction mixture was further refluxed for an extra 2 h. Thereafter, the solution was cooled and extracted three times with 30 ml portions of dichloromethane. The organic phase portions were mixed and dried by anhydrous $MgSO_4$, and after removing the solvent by means of evaporator, this afforded a brown oil. Yield: 245 mg, 72.4%. mp 145–147°C. IR(cm^{-1}) (C-H) 2959.5, (C=C) 1510.4, (Ar-N) 1433.0, (C-O) 123.5. ^{1}H NMR (600 MHz, $CDCl_3$, δ) 8.55 (m, 2H), 7.59 (m, 2H), 7.31 (m, 2H), 7.13 (m, 2H), 6.67 (dd, J = 91.8, 8.8 Hz, 4H), 4.39 (s, 4H), 3.85 (t, J = 6.6 Hz, 2H), 1.72–1.67 (q, 2H), 1.43 (m, 2H), 0.93 (t, J = 7.4 Hz, 3H). HRESI-MS $[M + Na]^+ m/z$ 370.2362 (calcd for $C_{22}H_{25}N_3ONa$ 370.4518).

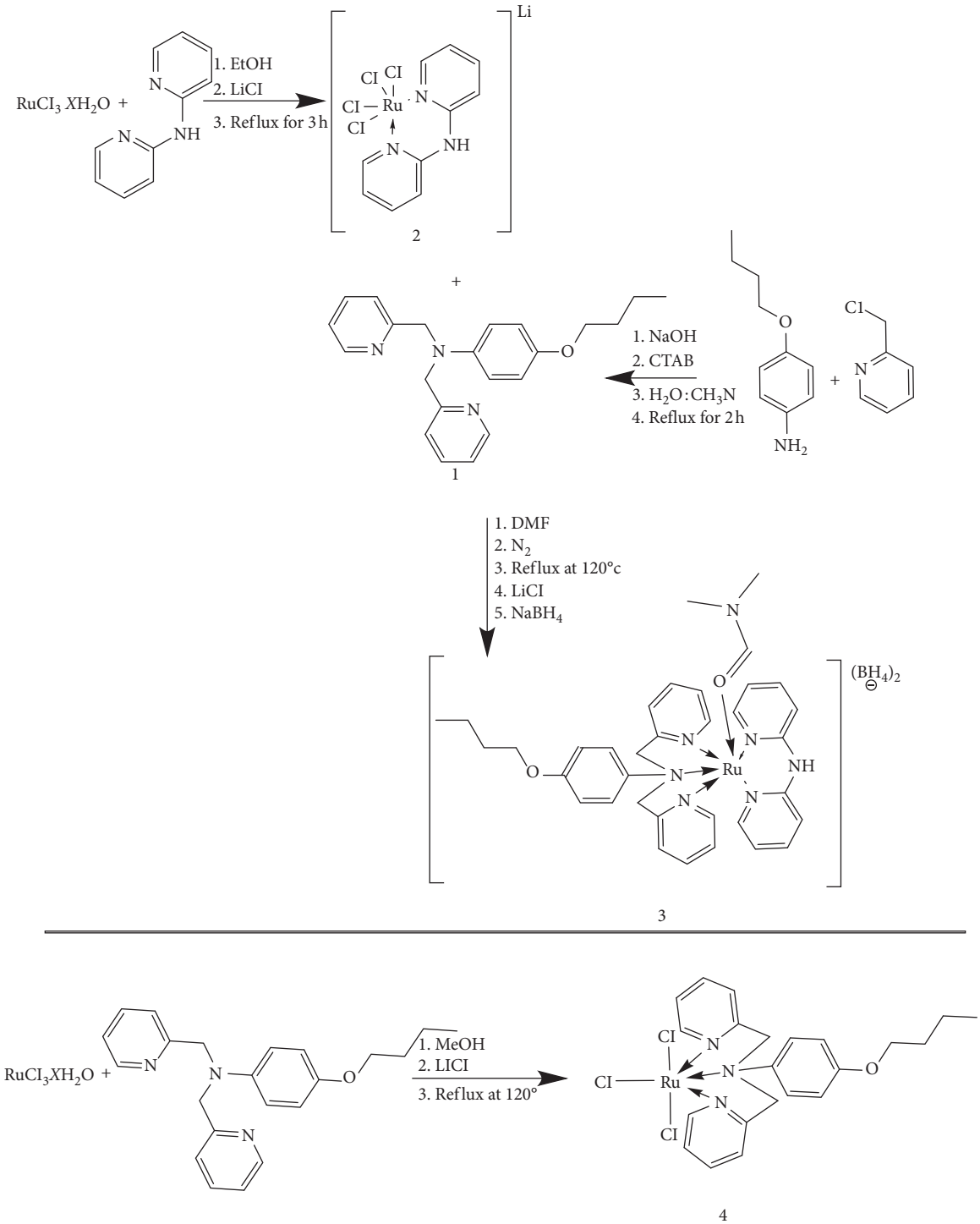

Figure 1: Synthetic routes for the ligand BUT **(2)** and ruthenium complexes: Li[Ru(Cl)$_4$(DPA)] **(1)**, [Ru(BUT)(DMF)(DPA)](BH$_4$)$_2$ **(3)**, and [Ru(BUT)(Cl)$_3$] **(4)**.

2.2.2. Preparation of Li[Ru(Cl)$_4$(DPA)] (2). Ruthenium trichloride trihydrate (1000 mg, 4.8 mmol) was mixed with 2,2-dipyridylamine (800 mg, 4.8 mmol) and lithium chloride (200 mg, 4.8 mmol) in 30 mL of absolute ethanol. The mixture was refluxed for 3 h at 120°C and filtered while it was still hot. The green precipitate formed was filtered by suction and washed with (3 × 30 ml) hot ethanol followed by (3 × 30 ml) diethyl ether. The product was afforded as a green powder. Yield: 1580 mg, 78.3%. IR (υ_{max}/cm^{-1}) (C-H) 3135.0, (C=C) 1534.0, (C-O) 1244.8, (Ar-N) 1431.2, (N-H) 3287.

1-3499.0. UV-Vis (DMF; λmax [nm]): 309, 373, 578. HRESI-MS [M + OH] m/z 439.3237 (calcd for $C_{10}H_{10}Cl_4LiN_3ORu$ 438.0157).

2.2.3. Preparation of [Ru(BUT)(DMF)(DPA)](BH$_4$)$_2$ (3). Lithium (tetrachloro)(dipyridylamine)ruthenate(III) **2** (170 mg, 0.40 mmol), (4-butoxy-*N*,*N*-bis(pyridin-2-ylmethyl) aniline 1 (140 mg, 0.40 mmol), and lithium chloride (170 mg, 0.40 mmol) were refluxed in 10 ml dimethylformamide for 3 h under nitrogen atmosphere at 120°C. The blue solution slowly turned dark blue during the reaction. The solution was cooled, and excess 30% sodium borohydride was added with stirring. The solution was extracted through liquid-liquid extraction to remove the excess dimethylformamide and to separate the product from the aqueous phase to the organic phase. The product was reddish and amorphous. Yield: 140 mg, 48.9%. IR (υ_{max}/cm^{-1}) (C-H) 2930.0, (C=C) 1504.0, (C-O) 1244.8, (Ar-N) 1434.2, (N-H) 3369.3, (C=O$_{DMF}$) 1950.1. UV-Vis (DMF; λmax [nm]): 297, 382, 596. HRESI-MS [M + NH$_4$] m/z 741.2516 (calcd for $C_{35}H_{53}B_2N_8O_2Ru^{2-}$ 741.3188).

2.2.4. Preparation of [Ru(BUT)(Cl)$_3$] (4). Ruthenium trichloride trihydrate (99.57 mg, 4.8 mmol) was mixed with 4-butoxy-*N*,*N*-bis (pyridin-2-ylmethyl)aniline 2 (166.6 mg, 4.8 mmol) and lithium chloride (200 mg, 4.8 mmol). The mixture was dissolved in 30 mL of absolute ethanol, then refluxed for 3 h at 120°C, and filtered while it was still hot. The deep brown precipitate formed was filtered by suction and washed with 30 ml of hot ethanol (3×) followed by 30 ml of diethyl ether (3×). The product obtained was a deep brown powder. Yield: 190 mg, 72.0%. IR (υ_{max}/cm^{-1}) (C-H) 2958.7, (C=C) 1503.8, (C-O) 1249.3, (Ar-N) 1438.3. UV-Vis (DMF; λmax [nm]): 271, 380, 596. HRESI-MS [M + K] m/z 593.1459 (calcd for $C_{22}H_{25}C_{l3}N_3OKRu$ 593.0107)

2.3. Antimicrobial Studies

2.3.1. Disc Diffusion Assay. This method was used and followed the National Committee for Clinical Laboratory Standards (NCCLS) as summarized in [26]. The antimicrobial susceptibility testing was performed using the disc diffusion method (sterile Whatman filter paper No. 6 [6 mm diameter]) on Mueller–Hinton (MH) agar in 90 mm Petri dishes. Bacterial inocula, with an incubation time not over 24 h, were adjusted to the standard solution of the 0.5 McFarland standard of 1.5×10^8 CFU/ml (colony forming units per millilitre) and inoculated with a sterile swab onto the surface of the culture medium. Soon thereafter, the plates were put to dry in an incubator at 35°C for 10 min. Whatman filter paper discs were saturated with 5 μl solutions of test compounds up to a concentration of 40 mg/ml. Five discs were put onto MH culture medium plate: one impregnated with acetonitrile solvent and four with test metal compounds. The distance from the centre of the disc to the next disc was maintained at a minimum of 20 mm, away from the plate edge. For the negative control, a Petri dish containing only the MH culture medium was included. For the quality control of the bacterial inoculum, at each bioassay, two Petri dishes containing standard antimicrobial discs were incubated with the quality control strains: *Staphylococcus aureus* (ATCC 25923), *Escherichia coli* (ATCC 25922), and *Klebsiella pneumonia* (ATCC 70063). The cultures were incubated at 35 ± 2°C for 18 h. After this period, the zones of inhibition including the diameter of the discs were measured. Inhibition zones above 7 mm in diameter were considered as positive results.

The minimal inhibitory concentration (MIC) was determined by broth microdilution method. Six concentrations of the metal compounds were made in serial dilution 2 : 1 (40, 20, 10, 5, 2.5, and 1.25) g/ml. Bacterial inocula, with an incubation time not over 24 h, were adjusted to the 0.5 McFarland standard and further diluted down to 5×10^5 CFU/ml by double distilled water. For the determination of the MIC, serial dilution was made in MH broth to a final volume of 100 μl in 96-well plates, and an aliquot of 100 μl of bacterial solution was added to each solution. The experiment was done using alamarBlue; this experiment shows a color change. In the color change, the MIC was observed as the first dilution without a color change from the blue solution. This was observed as the concentration of the metal compounds increases. The color change of the dye turns from blue to pink to indicate live microorganisms. The bioassays were performed in triplicate for accuracy. The bioassays were statistically evaluated using an ANOVA followed by T-test ($p < 0.05$).

2.3.2. Bacterial DNA Cleavage Assay. Cleavage of the bacterial DNA was determined by agarose gel electrophoresis to assess whether the compounds had any interaction with bacterial DNA. Ten microlitres of compounds that exhibited antimicrobial activities (40 μM) as determined in the disc diffusion assay were mixed with 10 μl of 53 μg/ml of the *S. aureus* DNA in Tris-HCl/NaCl buffer solution and then incubated at 37°C for 2 h. After this incubation, the samples were ran on 0.8% arose gel in Tris-acetic acid-EDTA buffer, at 60 V for 90 min. Then the gel was stained with ethidium bromide and photographed under 254 nm UV light.

3. Results and Discussion

3.1. Synthesis of the Ligand and the Corresponding Ru(II/III) Complexes. The ligand 4-butoxy-*N*,*N*-bis(pyridin-2-ylmethyl)aniline BUT 1 was synthesized through the alkylation of the amine moiety in 4-butoxyaniline by the picolinic arms from 2-chloromethyl pyridine. This alkylation is proposed to follow an SN_2 reaction mechanism. This is due to the use of a strong base sodium hydroxide, a primary alkyl-halide 2-chloromethyl pyridine, and the deprotonated (4-butoxyphenyl)nitride ion being a strong nucleophile. In this reaction, two moles of the base sodium hydroxide or in slight excess were used to deprotonate the protons from the amine moiety. Thereafter, the nucleophilic nitrogen attacks the carbocation on the two moles of the 2-chloromethyl pyridine. This then forms the BUT ligand. These changes can be observed spectroscopically through

FTIR. In FTIR, we observed the disappearance of the (NH_2) band from 4-butoxyaniline at stretching frequencies above 3000 cm^{-1} and the introduction of the pyridyl nitrogen band in the BUT ligand at 1474.3 cm^{-1}. This indicated that the picolinic arms were attached to the compound 4-butoxyaniline. Proton NMR showed the introduction of the aromatic multiplets at chemical shifts above 6 ppm in the BUT, and the peaks were due to the picolinic arms.

The three complexes were proposed to follow the dissociative mechanism on their formation reactions, due to the substitutive nature of the ligands during the reaction. The Ru(III) complex's starting reactant $RuCl_3.XH_2O$ has 3 water molecules within the coordination sphere, making it an octahedral complex. The nitrogen-based ligand reacting with $RuCl_3.XH_2O$ is also borderline basic and Ru(III) is more of a hard acid. Therefore, this reaction was still favored as this pair forms stronger bonds. In the reaction, chlorido ligands were proposed to dissociate and substitute with the pyridyl ligands. The Ru(II) complex was also proposed to follow the dissociative mechanism. The chlorido ligands were proposed to dissociate to create coordination binding sites for the pyridyl ligand. In this case, there was excess nitrogen-based ligand and the dimethylformamide solvent, thus forcing the ruthenium to become soft by reduction to Ru(II). There were many failed attempts to crystallize the complexes to grow a good crystal for single crystal XRD analysis; the only solution was to use the available HRESI-MS. As for the proton NMR, there was only one diamagnetic Ru complex which had poor solubility which only gave bad NMR spectra. The other complexes were Ru(III) and paramagnetic; thus their NMR showed diminished peaks or only the solvent peak. In this regard, we only resorted to using proton NMR for the ligand.

3.2. Characterization of the Ligand and the Corresponding Ru(II/III) Complexes

3.2.1. Vibrational Spectroscopy Characterization. The neat film IR of the compounds was recorded on a 4000 cm^{-1} to 150 cm^{-1} range, and tentative assignment of bands was done according to the proposed structures of the compounds. The spectral data showed that the BUT ligand was successfully formed. In analysis of this compound's FTIR data, the following expected functional groups were observed: the aliphatic (C-H) vibration at frequencies 2959.5 cm^{-1}; the aromatic (C=C) vibrations at frequencies 1510.4 cm^{-1}; and the (C-O) vibration which was a sharp and strong peak at 1235.5 cm^{-1}. These functional groups indicated the formation of the ligand but vibrations worth noting are the disappearance of the (-NH_2) vibration and the new pyridyl nitrogen vibration at vibrations of 1474.3 cm^{-1}.

The FTIR spectral data for the complexes showed that the ligands were coordinated. This is attributed to the observed decrease in vibrational frequencies of the coordinated donor atoms in the ligands. These vibrational frequencies are shown in Table 1. According to the binding nature of the metal to the ligands, there may be an increase or decrease in electron density towards the notable functional groups as per Hooke's law. Thus, this may show a lower or higher vibrational energy after coordination. This was observed in these complexes because the ruthenium centre pulls electrons inductively from the pyridyl nitrogen. This means that the carbon to nitrogen pyridyl bond will lose electron density, thus having a lower frequency of vibration. The spectra of the complexes showed a notable decrease in the pyridyl nitrogen vibrational frequency when the metal was introduced, thereby indicating complex formation.

3.2.2. Electronic Spectra and Magnetic Susceptibility. The electronic spectra of complexes below 300 nm showed charge transfer transitions and ligand transitions. These were labelled $\pi - \pi^*$ because pyridyl ligands are aromatic, hence have low lying vacant π orbitals. These were observed because of their high energy as seen by their appearances at shorter wavelengths and high intensities. All the transitions observed at energy above 500 nm were assumed to be the *d-d* transitions. In spectroscopy, *d-d* transitions are of low energy and should be observed at longer wavelengths. The electronic spectra results are summarized in Table 2. However, reports have shown that this can be observed even below 400 nm [27, 28]. The Ru(III) complexes had more chlorido ligands and a single bipyridyl ligand which meant that the bonds may not have been as strong as those having more nitrogen-based ligands. Thus, the transitions would be elongated due to the longer bonds of the ligands which ultimately give *d-d* transitions in the shorter wavelengths.

The electronic spectra of the Ru(III) complexes 2 and 4 showed simple yet ambiguous bands at the near IR site. In coordination chemistry, it is understood that, as the ligand orbitals approach the metal *d*-orbitals, there is split of the degeneracy of these metal orbitals. These are assumed to either distort or split in a regular octahedral field or a tetrahedral field. This means that there would be eg orbitals, which form the dz^2 and $dx^2 - y^2$ degenerate orbitals, and t_2g orbitals, which form the *dxy, dyz,* and *dxz* degenerate orbitals. Ruthenium, being a metal having 4*d*-orbitals, is known to have large *d*-orbitals. These large orbitals are known to have a smaller pairing energy. This means that these complexes would choose to assume a low spin field regardless of the ligand type. This was also indicated by the magnetic studies as these complexes were found to be d^5 low spin complexes.

Complex 2 had an effective magnetic moment of 1.63 BM which assumes a low spin d^5 Ru(III) complex. According to a low spin d^5 crystal field, we assigned the *d-d* transitions to 578 nm $^2T_{2g}(S) \longrightarrow {}^2T_{2g}$, $^2A_{2g}(I)$ and 373 nm $^2T_{2g}(S) \longrightarrow {}^2E_g(I)$ which are assumed to be the only energetically visible transitions from this complex. Complex 4 had an effective magnetic moment of 1.39 BM which still assumed a d^5 low spin Ru(III) complex. The significant deviation of the effective magnetic moment from the calculated spin-only magnetic moment is worth noting. Even though complexes 4 and 2 both have a ground term of *T* which assumes orbital contribution to their effective magnetic moment, it was observed to be a bit lower than the spin-only magnetic moment. This was assumed to be attributed to a high spin orbit coupling constant which may destroy the complexes

Table 1: Summarized FTIR assignments for ligands and complexes.

Compound	C-O (cm^{-1})	Ar-N (cm^{-1})	C=C (cm^{-1})	C-H (cm^{-1})	N-H (cm^{-1})
2,2-Dipyridylamine	0	1477.9	1529.42	3019.0	3179.33–3253.89
BUT *(1)*	1235.5	1474.3	1510.4	2959.5	0
$Li[Ru(Cl)_4(DPA)]$ *(2)*	0	1462.4	1534.5	3135.0	3287–3499
$[Ru(BUT)(DMF)(DPA)](BH_4)_2$ *(3)*	1244.8	1431.3	1504.0	2930.0	3369.3
$[Ru(BUT)Cl)_3]$ *(4)*	1249.3	1439.1	1608.2	2958.7	0

Table 2: Complexes and their associated electronic spectroscopy bands.

Transitions	$Li[Ru(Cl)_4(DPA)]$ *(2)* (nm)	$[Ru(BUT)(DMF)(DPA)](BH_4)_2$ *(3)* (nm)	$[Ru(BUT)(Cl)_3]$ *(4)* (nm)
$\pi - \pi^*$ and CT	<309	<271	<297
d-d	373, 578	356, 536	362, 542

CT: charge transfer bands.

paramagnetic behavior by aligning the orbit and the spin in opposite directions. This deviation was also assumed to be through weak Jahn-Teller distortions on these complexes' *d*-orbitals. The Ru(III) complexes 2 and 4 both had the pyridyl moiety. This moiety has many bonding interactions and thus generally makes these ligands above average in terms of strength in the spectrochemical series. The pyridyl moiety has an sp^2 hybrid lone pair of electrons in the aromatic nitrogen. This lone pair directly interacts with the *d*-orbitals of the metal, and this interaction has strong electrostatic interactions. Pyridine is also aromatic and has conjugated π bonds, and the pyridyl ring π electrons could also interact with the metal ions. The empty ring π orbitals can act as electron acceptors from the metal orbitals too. These π interactions happen because of the π orbital overlap with the metal *d*-orbitals. This suggested the weak Jahn-Teller distortions on Ru(III) complexes 2 and 4. Thus the assigned electronic bands for complex 4 are *d-d* transitions at 542 nm $^2T_{2g}(S) \longrightarrow {}^2T_{2g}$, $^2A_{2g}(I)$ and 362 nm $^2T_{2g}(S) \longrightarrow {}^2E_g(I)$, which still assumes a low spin d^5 crystal field as in complex 2. These were also assumed to be the energetically observable bands. The observed experimental transitions of these are summarized in Table 2.

Complex 3 on the contrary is a Ru(II) complex; this complex had an effective magnetic moment of <0 BM which assumed a d^6 low spin crystal field. According to this finding the suggested assigned transitions for this complex are the *d-d* transitions at 536 nm $^1A_{1g}(D) \longrightarrow {}^1T_{1g}(1)$ and 356 nm $^1A_{1g}(D) \longrightarrow {}^1T_{2g}(I)$. Other bands are very high in energy and would mostly be buried in the charge transfer bands and ligand bands.

3.2.3. Mass Spectrometry Analysis. In this study, the mass spectrometry used was electrospray ionization mass spectrometry (ESI-MS). This is important for the molecules studied as they are bulky molecules. Bulky molecules tend to fragment easily and are sometimes observed to fragment at the ion source rather than at the detector, hence making it difficult to measure the true molecular mass. The ESI-MS is a great choice as it is a soft ionisation technique and can avoid the immeasurable fragmentation that may be observed in other ionisation techniques in mass spectrometry. Complex 2 mass spectrum showed a diminished molecular ion peak at negative ion [M + OH] 439.3237 *m*/*z* which when subtracting the hydroxy is close to the calculated molecular mass of this complex 421.0130 amu. Considering the suspected fragments, the second intense peak at 378.9103 *m*/*z* was suspected to be the charged complex without the lithium cationic counterion. Most of the fragments were hard to assign as coordination compounds tend to isomerize and probably bind with other anions, thus forming new complexes. Computational calculations that predict fragments would help in this regard. However, the fragment that might be due to the ligand 2,2-dipyridylamine (DPA) was observed at [DPA + 2H] 173.1267 *m*/*z*. The peaks observed on the spectrum had a ruthenium isotropic pattern, which confirmed the presence of ruthenium in the compound, and this validation may conclude that this complex was successfully characterized. Complex 4 showed the ruthenium isotropic pattern. This molecule showed a corroborative molecular ion peak to the molecular mass of the complex. The positive ion [M + K] was suspected to be observed at 593.1459 *m*/*z* while the molecular mass for the complex with potassium was calculated to be 593.0107 amu. Complex 3 mass spectrum also had corresponding peaks with the ruthenium isotropic pattern. This molecule's molecular ion peak was observed at positive ion $[M + NH_4]$ 741.2516 *m*/*z*. This corresponds to a molecular mass of complex 3 with ammonium to be 741.3188 amu. This molecule also had challenging fragments to assign noticeable fragments. In this regard, they were not physically assigned. However, the DPA fragment was suspected to be observed at [DPA + H] 172.1294 *m*/*z*. Table 3 summarizes the experimental and calculated molecular masses of the synthesized complexes.

3.3. Antibacterial Activity by Disc Diffusion and MIC Assays. Antibacterial studies were performed on four bacterial species: *S. aureus, K. pneumoniae*, MRSA, and MDR *K. pneumoniae*. All compounds, $Li[Ru(Cl)_4(DPA)]$ 2, $[Ru(BUT)(DMF)(DPA)](BH_4)_2$ 3, $[Ru(BUT)(Cl)_3]$ 4, 2,2-dipyridylamine, and BUT 1, were screened at a final concentration of 40 μM. The disc diffusion assay showed broad range activity against both Gram-positive and Gram-negative species, with more activity observed for the

Table 3: Experimental and calculated mass of complexes.

Compound	Experimental (m/z)	Calculated (amu)
$Li[Ru(Cl)_4(DPA)]$ *(2)* [M + OH]	439.3237	438.0157
$[Ru(BUT)(DMF)(DPA)](BH_4)_2$ *(3)* [M + NH_4]	741.2516	741.3188
$[Ru(BUT)(Cl)_3]$ *(4)* [M + K]	593.1459	593.0107

Gram-positive. There was more activity observed for the nonresistant strains *S. aureus* and *K. pneumoniae* (Table 4). It was also observed that some compounds had activity against the drug resistance MRSA species. However, there was no activity from any of the compounds against MDR *K. pneumoniae*.

The results of the nonresistant species *K. pneumoniae* showed good activity from all compounds. The activity ranged from 7 mm to 12 mm, with 2,2-dipyridylamine having the highest activity. With this exceptional bioactivity from this ligand, it could be inferred that, upon introduction of the metal centre, the activity reduced compared to complexes 2 and 3 which had a zone of 7 mm. The inference that could be made from all compounds having activity against *K. pneumoniae* except its resistant strain is that these new synthetic compounds have a similar route of mechanism to the nonresistant strain. In this regard, the new compounds did not have activity towards the MDR *K. pneumoniae* strain. In terms of *S. aureus,* there was overall activity from all compounds. However, there was an observed potent activity coming from complex 3 which had an inhibition zone of 18 mm. In terms of MRSA, there was activity from all the ligands except the complexes. The inference for this observation may be that when the BUT 1 and 2,2-dipyridylamine ligands were coordinated to ruthenium, their bioactivity towards MRSA was disabled. This observation suggests that coordinated BUT 1 and 2,2-dipyridylamine ligands may be affected by the virulent *mecA* gene. The *mecA* gene is the main mode of resistance of this organism [29]. These active ligands may have a novel mechanism or more mechanisms of action towards MRSA. The zones of inhibition for all compounds are given in Table 4 below.

The MIC was used to assess the lowest concentration of the active compounds that can stop either the growth or the reproduction of the bacterial species. The data from this assay also showed that the Gram-positive bacterial species had more activity. This was observed from their general trend which shows larger zones of inhibition and lower MICs, while for the Gram-negative *K. pneumoniae* there is higher MICs and smaller zones of inhibition. This was suspected to be because of the difference in the Gram-negative bacterial membranes compared to the Gram-positive ones. Gram-negative cell membranes use the porin or efflux pump for ingestion and excretion [30]. This efflux pump/porin may exclude certain foreign objects from entering the bacterial cell. It is assumed that these porins may be too small to accommodate some compounds or reject some compounds because of their biochemical nature. This suggested that the compounds' concentration in the cell's cytoplasm would be too little or there would not be any of the compounds, hence making them ineffective in the target. This suggested the observation of the compounds being more effective on the Gram-positive bacteria because of their less restrictive outer membrane [31]. The MIC results showed that some of the compounds are either bactericidal or bacteriostatic. Bactericidal compounds kill the bacteria and this was observed at MICs that were below 4 mg/ml. Bacteriostatic compounds stop the reproduction of the bacterial organisms, and this was observed at MICs that were above 4 mg/ml [32]. The MIC results are given in Table 5 after calculations from the coulometric study.

It was observed that the complexes generally have lower MIC values compared to their free ligands. However, the BUT ligand showed exceptional results against *S. aureus*, where its complex was observed to have higher MICs. The ligands which were active against MRSA showed that a higher concentration was needed for their activity against this resistant strain.

3.4. Gel Electrophoresis Assay. Metal complexes have some affinity to nucleic acids, and it has been reported that nucleic acids are the most likely target for these [33–35]. In this study, we observed from the disc diffusion and MIC assays that all the synthesized compounds had activity towards the nonresistant strains and the drug-resistant MRSA. Gel electrophoresis is a tool that helps in identifying or studying the fragmentation of nucleic acids due to interaction with an external factor. This tool was employed to assess the kind of interaction the compounds might have with the DNA. The DNA used was 53 μg/ml of *S. aureus* organism. The DNA was freshly extracted and treated with the compounds before running the gel. Figure 2 shows the interaction of these compounds with this DNA.

The first lane was of the DNA marker. The second lane marked with C was of the untreated DNA to be compared with wells of the treated DNA. The lanes containing the complexes (Lanes 1, 5, and 7) showed that the DNA was completely denatured. These complexes showed complete chemical nuclease effect because there was no observed band or forms of the DNA. This was assumed to be because of strong affinity of these complexes towards DNA. All these complexes have planar heterocyclic ligands, and ligands of this nature are known to induce DNA cleavage by intercalation. The intercalation of the ligands coupled with the reactivity of the metal centre may also explain why there is complete nuclease activity and DNA denaturing. The Ru(II) complexes had the dimethylformamide as a ligand. This ligand is labile and may be replaced by any stronger ligand; this includes biomolecules such as the DNA with its abundant donor atoms (sulphur, oxygen, nitrogen, and phosphorus). This was still the case for the Ru(III) complexes as they have labile chlorido ligands. This means that it is possible that these labile ligands may be displaced by the donor atoms found in the genomic material. This could lead

Table 4: Average zones of inhibition of all compounds.

Microbe	$Li[Ru(Cl)_4(DPA)$ (*2*) (mm)	$[Ru(BUT)(DMF)(DPA)](BH_4)_2$ (*3*) (mm)	$[Ru(BUT)(Cl)_3]$ (*4*) (mm)	BUT (*1*) (mm)	2,2-Dipyridylamine (mm)
S. aureus	9	18	7	8	9
MRSA	0	0	0	8	7
K. pneumoniae	7	7	7	12	7
MDR *K. pneumoniae*	0	0	0	0	0

Table 5: MIC of all active compounds.

Microbe	$Li[Ru(Cl)_4(DPA)$ (*2*) (mg/ml)	$[Ru(BUT)(Cl)_3]$ (*4*) (mg/ml)	$[Ru(BUT)(DMF)(DPA)](BH_4)_2$ (*3*) (mg/ml)	2,2-Dipyridylamine (mg/ml)	BUT (*1*) (mg/ml)
S. aureus	5.00	10.00	1.88	15.00	0.03
MRSA	0	0	0	15.00	30.00
K. pneumoniae	10.00	10.00	15.00	1.88	20.00
MDR *K. pneumoniae*	0	0	0	0	0

0: not active.

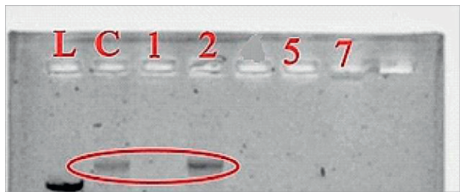

Figure 2: DNA cleavage analysis on 0.8% agarose gel. Lane **L**: 1 kb ladder; **C**: control DNA; **1**: complex 2; **2**: BUT; **5**: complex 4; **7**: complex 3.

to strong interactions that lead to complete damage of the genomic material [36–38]. This strong interaction completely disrupts the conformation of the DNA and the bonds that make up the DNA polymer where now the base pairs are no longer bound together. If this inference is true, then the damaged DNA will not be observed in the gel. This suggests that the mode of action includes DNA damage by the complexes.

The ligand BUT on Lane 2 was observed not to cleave DNA in any way. However, these molecules showed good zones of inhibition for *S. aureus*, *K. pneumoniae*, and MRSA. These findings suggest that this ligand may have had a different mode of action contrary to complexes. This can also be inferred from the enabling and disabling chemistry observed where ligands may have activity or no activity once a metal is introduced. This also suggested that the introduction of a metal induced a different mode of action or multiple modes of action towards the bacteria. The mode of action against these bacterial organisms was assumed to be through DNA chemical nuclease activity. However, this was not the case for the BUT 1 ligand. This should be confirmed by employing other assays to rule out any other possibilities or other modes of action these compounds might have.

4. Conclusions

The results of this work showed that the 3 complexes were successfully synthesized. This was observed from their spectroscopic FTIR and UV/Vis data. From FTIR, important functional groups in the near IR were observed, and those that were for the metal to ligand bonds showed a decrease in frequency which indicated coordination. The electronic spectra data also showed the electronically allowed and energetically observable transitions which suggested low spin d^5 and d^6 complexes of Ru(III) and Ru(II), respectively. This was corroborated with their magnetic susceptibility studies which suggested the same inference. The ligands and complexes ESI-MS experiments were done to assess their molecular formula; the results showed that the suggested molecular masses were obtained for all the compounds. The preliminary antibacterial assays showed that complexes and ligands were more active against the nonresistant strains *S. aureus* and *K. pneumoniae,* with more activity towards the Gram-positive species. As for the resistant strains, there was no activity towards MDR *K. pneumoniae* while there was activity towards MRSA from the two ligands 2,2-dipyridylamine and BUT only. The gel electrophoresis DNA binding of these complexes showed nucleation of the DNA from the complexes and no interaction from the ligands. This suggested that one of the modes of action of the complexes was through DNA denaturing.

Data Availability

The characterization and biological assay data used to support the findings of this study are summarized within the article in Section 2.1 and in tables. In addition, the Supplementary Materials include the spectral data of the compounds.

Conflicts of Interest

The authors declare that they have no conflicts of interest.

Acknowledgments

This work was financially supported by Botswana International University of Science and Technology Initiation

Grants and University of Botswana Office of Research and Development.

Supplementary Materials

1. 4-Butoxy-*N*,*N*-bis(pyridin-2-ylmethyl)aniline (BUT) 1 Supplementary Material: Figure 1: proton NMR spectrum of BUT 1. Figure 2: FTIR spectrum of BUT 1. Figure 3: HRESI-MS spectrum of BUT 1.2. Li[Ru(Cl)4(DPA)] 2 Supplementary Material: Figure 4: FTIR spectrum of complex 2. Figure 5: UV/Vis spectrum of complex 1. Figure 6: HRESI-MS spectrum of complex 2.3. [Ru(BUT)(DMF)(DPA)]$(BH_4)_2$ 3 Supplementary Material: Figure 7: FTIR spectrum of complex 3. Figure 8: UV/Vis spectrum of complex 3. Figure 9: HRESI-MS spectrum of complex 3.4. [Ru(BUT)(Cl)3] 4 Supplementary Material: Figure 10: FTIR spectrum of complex 4. Figure 11: UV/Vis spectrum of complex 4. Figure 12: HRESI-MS spectrum of complex 4. (*Supplementary Materials*)

References

[1] K. Lewis, "Platforms for antibiotic discovery," *Nature Reviews Drug Discovery*, vol. 12, no. 5, pp. 371–387, 2013.

[2] J. L. Clement and P. S. Jarrett, "Antibacterial silver," *Metal-Based Drugs*, vol. 1, no. 5-6, pp. 467–482, 1994.

[3] H. Zhang, F. Yang, Q. Wu et al., "Synthesis, DNA-binding properties and quantitative structure-activity relationships on ruthenium(II) complexes with calf-thymus DNA," *Medicinal Chemistry*, vol. 6, no. 3, 2016.

[4] H. R. Barai, D. J. Lee, S. W. Han, and Y. J. Jang, "Interaction and binding modes of bis-ruthenium(II) complex to synthetic DNAs," *Metals*, vol. 6, no. 6, p. 141, 2016.

[5] N. E. A. El-Gamel and A. M. Fekry, "Antimicrobial ruthenium complex coating on the surface of titanium alloy. high efficiency anticorrosion protection of ruthenium complex," *Bioelectrochemistry*, vol. 104, pp. 35–43, 2015.

[6] H. M. Southam, J. A. Butler, J. A. Chapman, and R. K. Poole, "The microbiology of ruthenium complexes," *Advances in Microbial Physiology*, vol. 71, pp. 1–96, 2017.

[7] Y. Yang, G. Liao, and C. Fu, "Recent advances on octahedral polypyridyl ruthenium(II) complexes as antimicrobial agents," *Polymers*, vol. 10, no. 6, p. 650, 2018.

[8] F. Li, J. G. Collins, F. R. Keene, and F. R. Keene, "Ruthenium complexes as antimicrobial agents," *Chemical Society Reviews*, vol. 44, no. 8, pp. 2529–2542, 2015.

[9] C. S. Allardyce and P. J. Dyson, "Ruthenium in medicine: current clinical uses and future prospects," *Platinum Metals Review*, vol. 45, no. 2, pp. 62–69, 2001.

[10] D. Thompson, "The chemistry of precious metals by S.A. cotton," *Gold Bulletin*, vol. 31, no. 1, p. 35, 1998.

[11] B. Norden, P. Lincoln, and B. Akerman, "Transition metal ion complexes. Metal ions in biological systems," in *Probing of Nucleic Acids by Metal Ion Complexes of Small Molecules*, p. 177, CRC Press, Boca Raton, FL, USA, 1996.

[12] N. W. Luedtke, J. S. Hwang, E. Nava, D. Gut, M. Kol, and Y. Tor, "The DNA and RNA specificity of eilatin Ru(II) complexes as compared to eilatin and ethidium bromide," *Nucleic Acids Research*, vol. 31, no. 19, pp. 5732–5740, 2003.

[13] S. H. Sumrra and Z. H. Chohan, "Antibacterial and antifungal oxovanadium(IV) complexes of triazole-derived Schiff bases," *Medicinal Chemistry Research*, vol. 22, no. 8, pp. 3934–3942, 2013.

[14] K. V. Kumar, K. Sunand, K. Ashwini, P. S. Kumar, S. Vishnu, and A. Samala, "Synthesis characterization and antibacterial studies of 4-aminoantipyrine schiff's bases," *International Journal of Applied Pharmaceutical Sciences and Research*, vol. 2, no. 1, 2016.

[15] Z. H. Chohan and M. Hanif, "Antibacterial and antifungal metal based triazole Schiff bases," *Journal of Enzyme Inhibition and Medicinal Chemistry*, vol. 28, no. 5, pp. 944–953, 2013.

[16] A. Goszczyńska, H. Kwiecień, and K. Fijałkowski, "Synthesis and antibacterial activity of schiff bases and amines derived from alkyl 2-(2-formyl-4-nitrophenoxy)alkanoates," *Medicinal Chemistry Research*, vol. 24, no. 9, pp. 3561–3577, 2015.

[17] R. Abarca, G. Gomez, C. Velasquez et al., "Antibacterial behavior of pyridinecarboxylatesilver(I) complexes," *Chinese Journal of Chemistry*, vol. 30, no. 7, pp. 1631–1635, 2012.

[18] R. Saddik, A. Gaadaoui, A. Hamal, A. Zarrouk, R. Touzani, and N. Benchat, "Synthesis, antibacterial and antifungal activity of some new imidazo[1,2-a]pyridine derivatives," *Der Pharmacia Lettre*, vol. 6, no. 4, 2014.

[19] K. R. Lakomehsari, S. T. Ganjali, R. Zadmard, and M. Roshan, "A novel azo-calixaren derivative based on 2,6-diamino pyridine: synthesis, characterization and antibacterial evaluation," *Letters in Organic Chemistry*, vol. 14, no. 4, pp. 300–304, 2017.

[20] J. Y. Chen, X. X. Ren, Z. W. Mao, and X. Y. Le, "Synthesis, characterization, and antibacterial activities of two new copper(II) glycinate complexes incorporating 2-(4′-thiazolyl) benzimidazole/2-(2-pyridyl)benzimidazole," *Journal of Coordination Chemistry*, vol. 65, no. 12, pp. 2182–2191, 2012.

[21] S. Sangilipandi, D. Sutradhar, K. Bhattacharjee et al., "Synthesis, structure, antibacterial studies and DFT calculations of arene ruthenium, Cp∗Rh, Cp∗Ir and tricarbonylrhenium metal complexes containing 2-chloro-3-(3-(2-pyridyl)pyrazolyl)quinoxaline ligand," *Inorganica Chimica Acta*, vol. 441, pp. 95–108, 2016.

[22] I. L. Mawnai, S. Adhikari, L. Dkhar, J. L. Tyagi, K. M. Poluri, and M. R. Kollipara, "Synthesis and antimicrobial studies of half-sandwich arene platinum group complexes containing pyridylpyrazolyl ligands," *Journal of Coordination Chemistry*, vol. 72, no. 2, pp. 294–308, 2019.

[23] V. Balzani and A. Juris, "Photochemistry and photophysics of Ru(II)-polypyridine complexes in the Bologna group. From early studies to recent developments," *Coordination Chemistry Reviews*, vol. 211, no. 1, pp. 97–115, 2001.

[24] B. G. Tweedy, "Possible mechanism for reduction of elemental sulfur by *Monilinia fructicola*," *Phytopathology*, vol. 55, pp. 910–914, 1964.

[25] A. D. Richards and A. Rodger, "Synthetic metallomolecules as agents for the control of DNA structure," *Chemical Society Reviews*, vol. 36, no. 3, pp. 471–483, 2007.

[26] K. Lalitha, "Manual on antimicrobial susceptibility testing," in *Performance Standards for Antimicrobial Testing: Twelfth Informational Supplement*, vol. 56238, pp. 454–456, Clinical and Laboratory Standards Institute, Wayne, PA, USA, 2004.

[27] P. T. Manoharan, P. K. Mehrotra, M. M. Taquikhan, and R. K. Andal, "Optical and magnetic properties and geometry of some d5 ruthenium complexes," *Inorganic Chemistry*, vol. 12, no. 12, pp. 2753–2757, 1973.

[28] G. Bryant, J. Fergusson, and H. Powell, "Charge-transfer and intraligand electronic spectra of bipyridyl complexes of iron, ruthenium, and osmium. I. Bivalent complexes," *Australian Journal of Chemistry*, vol. 24, no. 2, pp. 257–273, 1971.

[29] C. Walsh, "Molecular mechanisms that confer antibacterial drug resistance," *Nature*, vol. 406, no. 6797, pp. 775–781, 2000.

[30] J. L. Martínez and F. Baquero, "Emergence and spread of antibiotic resistance: setting a parameter space," *Upsala Journal of Medical Sciences*, vol. 119, no. 2, pp. 68–77, 2014.

[31] A. Weseler, H. K. Geiss, R. Saller, and J. Reichling, "A novel colorimetric broth microdilution method to determine the minimum inhibitory concentration (MIC) of antibiotics and essential oils against *Helicobacter pylori*," *Ie Pharmazie-An International Journal of Pharmaceutical Sciences*, vol. 60, no. 7, pp. 498–502, 2005.

[32] M. A. Hachem, J. M. Andersen, R. Barrangou et al., "Recent insight into oligosaccharide uptake and metabolism in probiotic bacteria," *Biocatalysis and Biotransformation*, vol. 31, no. 4, pp. 226–235, 2013.

[33] R. Sharma, "Synthesis, characterization, antimicrobial and DNA cleavage studies of transition metal complexes of 4-(triflouro-4-ylidene)hydrazinecarbothioamide," *International Journal of Applied Biology and Pharmaceutical Technology*, vol. 20, no. 4, 2013.

[34] R. M. Anil, E. Shanmukhappa, B. Rangaswamy, and M. Revanasiddappa, "Synthesis, characterization, antimicrobial activity, antifungal activity and DNA cleavage studies of transition metal complexes with schiff base ligand," *International Journal of Innovative Research in Science, Engineering and Technology*, vol. 4, no. 2, pp. 60–66, 2015.

[35] S. Bargotya, N. Mathur, and A. K. Sharma, "Anti microbial & DNA cleavage studies of heterocyclic metal complexes," 2018, https://morebooks.de/store/pt/book/anti-microbial-dna-cleavage-studies-of-heterocyclic-metal-comlexes/isbn/978-613-8-34627-2.

[36] Y. Sindhu, C. J. Athira, S. M. Sujamol, R. S. Joseyphus, and K. Monahan, "Synthesis, characterization, DNA cleavage, and antimicrobial studies of some transition metal complexes with a novel schiff base derived from 2-aminopyrimidine," *Synthesis and Reactivity in Inorganic Metal-Organic and Nano-Metal Chemistry*, vol. 43, no. 3, pp. 226–236, 2013.

[37] V. Brabec, J. Pracharova, J. Stepankova, P. J. Sadler, and J. Kasparkova, "Photo-induced DNA cleavage and cytotoxicity of a ruthenium(II) arene anticancer complex," *Journal of Inorganic Biochemistry*, vol. 160, pp. 149–155, 2016.

[38] C. Griffith, A. S. Dayoub, T. Jaranatne et al., "Cellular and cell-free studies of catalytic DNA cleavage by ruthenium polypyridyl complexes containing redox-active intercalating ligands," *Chemical Science*, vol. 8, no. 5, pp. 3726–3740, 2017.